Measurements of Silicon Photomultipliers Responsivity in Continuous Wave Regime

Gabriele Adamo, Diego Agrò, Salvatore Stivala, Antonino Parisi, Giuseppe Costantino Giaconia, Alessandro Busacca, Massimo Mazzillo, Delfo Sanfilippo, and Giorgio Fallica

***Abstract*— We report on the electrical and optical characterization, in continuous wave regime, of a novel class of silicon photomultipliers fabricated in standard planar technology on a silicon *p*-type substrate. Responsivity measurements, performed with an incident optical power down to tenths of picowatts, at different reverse bias voltages and on a broad (340–820 nm) spectrum, will be shown and discussed. The device temperature was monitored, allowing us to give a physical interpretation of the measurements. The obtained results demonstrate that such novel silicon photomultipliers are suitable as sensitive power meters for low photon fluxes.**

***Index Terms*— Avalanche photodiode (APD), photodetector, responsivity, silicon photomultiplier (SiPM), single-photon avalanche diode (SPAD).**

I. Introduction

CURRENT research in photodetectors is directed toward an increasing miniaturization of the pixel size, thus both improving the spatial resolution and reducing the device dimensions. On the other hand, measurements of low photon fluxes require high responsivity. In this scenario, silicon photomultipliers (SiPMs) emerge as promising candidates and are considered an attractive possibility to replace both standard vacuum photomultiplier tubes (PMTs) and conventional avalanche photodiodes (APDs). SiPMs are large area detectors consisting of a parallel array of Geiger Mode APDs with individual integrated quenching resistors [1], [2]. Each photodiode is an independent photon counting microcell and is connected to a common analog output to produce a summation signal [3], [4] proportional to the number of detected photons [5]–[7]. If compared with standard vacuum PMTs, SiPMs show higher quantum efficiency, especially in the near infrared, low operating voltage ($<$30 V) with a comparable gain ($>10^6$), ruggedness, compact size, and reduced sensitivity with temperature, voltage fluctuations, and magnetic fields [6]–[12]. Furthermore, solid-state technology owns the typical advantages of the planar integration process: SiPMs can be manufactured at lower costs and with higher reproducibility with respect to PMTs [13], [14]. SiPMs show several advantages compared with APDs fabricated in conventional CMOS technology [15], such as: low bias voltage, higher responsivity, and photon detection efficiency in the visible and near infrared range, excellent single-photon response, fast rise time ($\ll$1 ns), and low power consumption. Moreover, SiPMs have a much higher gain than APDs ($>10^6$ versus $<10^3$) [5]. Also, with reference to the integration process, they can be used in medical imaging systems like positron emission tomography, magnetic resonance imaging [16]–[19], near-infrared spectroscopy (e.g., oximetry) [20], [21], and in immunoassay tests [22]. On the other hand, features like their high gain, fast timing response with low fluctuation and high responsivity to extremely low photon fluxes [14] could open up new SiPMs applications in a variety of fields, such as very low power measurements (less than 1 pW) [23]. SiPMs performances in photon counting mode have been investigated in several papers, using picosecond pulsed lasers [1]–[3], [8]–[14], [24]. Optical characterization performed via continuous wave (CW) sources has seldom been reported [23], [25] even though this kind of excitation seems to be very useful in several applications [22], [23], [26]–[30].

In this paper, we report on the electrical and CW optical characterization of a novel class of SiPMs fabricated in standard silicon planar technology. We will show the results of our responsivity measurements carried out on the 340–820-nm spectrum, at different reverse bias voltages and incident optical power values.

II. Device Description

SiPM fabrication technology is based on single-photon avalanche diode (SPAD) cells. The device has a breakdown voltage of about 28.0 V and a 3.5 mm $\times$ 3.5 mm active area (3600 microcells, 45% fill factor, and 58-μm cell pitch) enclosed in a 5-mm $\times$ 5.5-mm package. Fig. 1 shows a sketch of the device cross section, while in Fig. 2 an optical microscopy image of the large area SiPM investigated in this paper is reported. An n-p junction is fabricated on silicon epitaxial p-type wafers through a planar process and it operates with a reverse biased voltage, well above the breakdown value (Geiger mode).

Manuscript received July 30, 2012; revised May 3, 2013 and July 3, 2013; accepted September 16, 2013. Date of publication October 1, 2013; date of current version October 18, 2013. This work was supported by the Telecom Italia for the Ph.D. program of D. Agrò. The review of this paper was arranged by Editor S. Ralph.

G. Adamo, D. Agrò, S. Stivala, A. Parisi, G. C. Giaconia, and A. Busacca are with the Department of Energy, Information Engineering and Mathematical Models, University of Palermo, Palermo 90128, Italy (e-mail: gabriele.adamo@unipa.it; diego.agro@unipa.it; salvatore.stivala@unipa.it; antonino.parisi@unipa.it; costantino.giaconia@unipa.it; alessandro.busacca@unipa.it).

M. Mazzillo, D. Sanfilippo, and G. Fallica are with the Research and Development IMS, STMicroelectronics, Catania 95121, Italy (e-mail: massimo.mazzillo@st.com; delfo.sanfilippo@st.com; giorgio.fallica@st.com).

Color versions of one or more of the figures in this paper are available online at http://ieeexplore.ieee.org.

Digital Object Identifier 10.1109/TED.2013.2282709

0018-9383 © 2013 IEEE

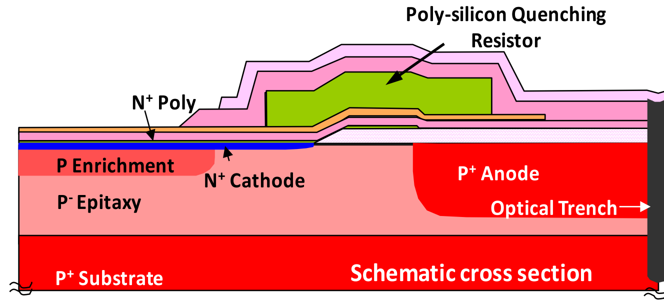

Fig. 1. Schematic cross section of the SiPM cell.

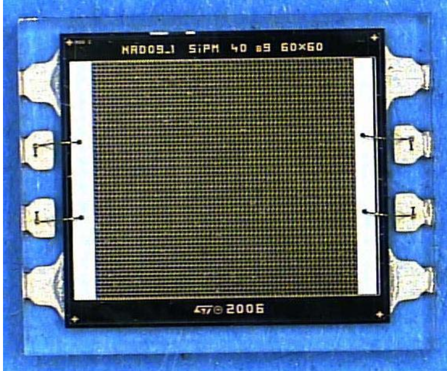

Fig. 2. Optical microscopy picture of the large area SiPM in SMD package.

The anode is defined through a boron implanted p-layer that forms an enrichment region in every microcell, thus fixing the junction breakdown voltage. The anode is surrounded by an implanted p^+ sinker that is connected to a bonding pad; hence it can be biased either from the back side or from the front side. The cathode is a 0.2-μm thin n^+ polysilicon layer, doped with an arsenic diffusion, deposited on the top of the structure [31].

The quenching circuit is passive and made of a low-doped polysilicon resistor. The latter is present in every single cell, in the form of a transparent square frame integrated on the top of the cathode [30] and has a value of 256 kΩ (such measurement is reported in Section III-A). Other features of the fabricated devices are: a thin junction depletion layer (about 1-μm thick, corresponding to a breakdown voltage of about 28.0 V); a reduced thickness (about 0.15 μm) of the quasi-neutral region above the space charge region, to increase the absorption efficiency in the blue wavelength range; a suitable structure for optical isolation consisting of thin trenches (1-μm wide) filled with tungsten and silicon oxide surrounding the active area of each microcell [31]. Moreover, dedicated gettering techniques have been integrated into the manufacturing process to reduce the defectivity in the active area [14].

Emission microscope pictures with different magnification, reported in Fig. 3, show the avalanche turn-on phase in a typical SiPM kept in dark condition and reverse biased at 3 V above the breakdown voltage. Such images were acquired using a Hamamatsu PHEMOS-1000 photon emission microscope and applying a positive voltage to the SiPM common cathode metallization, while the anode metallization was set at ground.

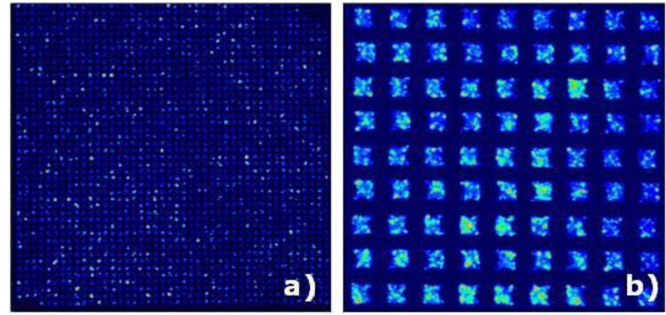

Fig. 3. Emission microscope pictures with (a) low and (b) high magnification factor obtained on a 3.5-mm × 3.5-mm SiPM reverse biased at 3 V above the breakdown voltage.

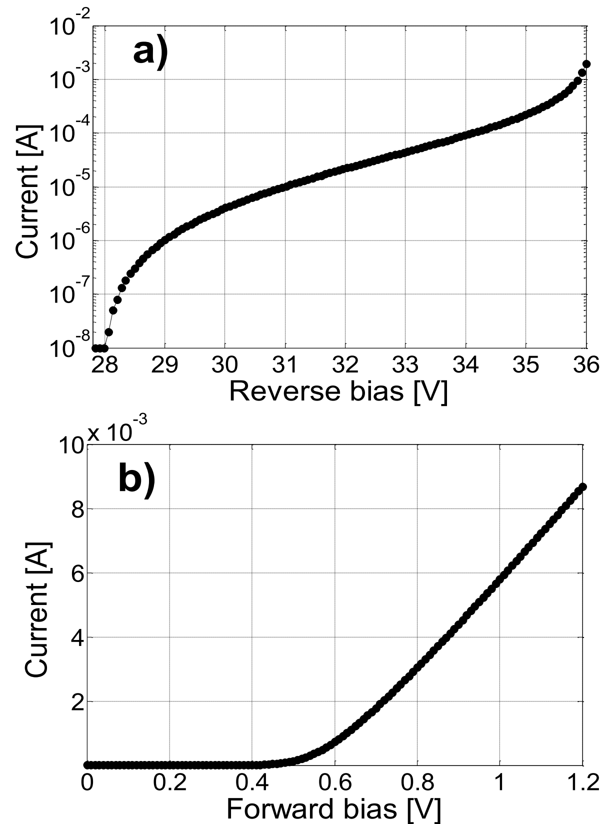

Fig. 4. (a) Reverse and (b) forward I–V SiPM characteristics measured at room temperature and in dark conditions.

III. Experimental Results and Data Analysis

A. Electrical Characterization

Measurements of SiPM forward and reverse current and breakdown voltage were performed using a semiconductor parameter analyzer (Keithley 2440) at controlled room temperature and in dark conditions. We found a breakdown voltage of 28.0 V [Fig. 4(a)]. A linear behavior of the I–V characteristic (on a semilogarithmic scale) was detected from 30.0 to 35.3 V (OV = 7.3 V, i.e., 26% above the breakdown voltage). In forward bias, the current is limited by the quenching resistor [32]. Therefore, its value can be extrapolated from the forward I–V characteristic in Fig. 4(b). The slope of the linear region provided a value of 71 Ω

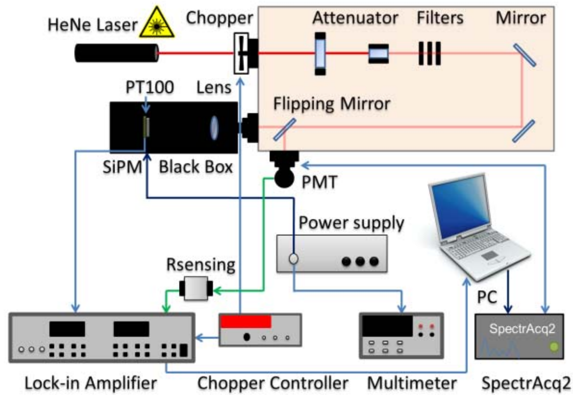

Fig. 5. Sketch of the experimental setup for measurements of SiPM responsivity versus incident optical power.

for the overall SiPM quenching resistor that corresponds to a quenching resistor of 256 kΩ for each single microcell.

B. Measurements of Responsivity as a Function of the Incident Optical Power

Herein, we refer to responsivity as the ratio of the SiPM output current (net of the dark current) and the incident optical power and it is not normalized to the SiPM gain. To explore the linear behavior of the device, we first performed SiPM responsivity measurements as a function of the incident optical power. The experimental setup is shown in Fig. 5. The optical power provided by a HeNe laser ($\lambda = 632.8$ nm) was attenuated using some neutral density filters and controlled through a half-wave plate and a Glan–Thompson cube polarizer. This system allowed us to fine tune the optical power down to sub picowatts. The laser beam was chopped at 183 Hz and was sent—depending on the position of a flipping mirror—either on the active area of the SiPM under test or on a reference PMT (Hamamatsu R928), previously calibrated and used to estimate the optical power incident on the SiPM.

The latter was biased using a stabilized power supply and a SMD resistor (100 Ω, sensing resistor), connected between the cathode and the ground. Unlike what several papers report for pulsed measurements [11], [14], we did not include any other resistor in the bias line. This resistor, together with the capacitors of the SiPM itself (or capacitors eventually present in the biasing circuit), could behave as a low-pass filter for the SiPM response. This would limit the linear response of the device, when working in the CW regime and on a wide range of incident optical powers.

The SiPM and the biasing circuit were located in a metal black box, being thus shielded by ambient light and electromagnetic noise. A 25-mm focal length lens was placed between the flipping mirror and the SiPM, making sure that the light spot covered the whole active area of the device. During measurements, the temperature of the SiPM package was monitored with a PT100 thermistor placed in the back side of the device. To perform low optical power measurements, a lock-in amplifier was connected to both the SiPM and the PMT outputs, while a readout system (SpectrAcq2) digitalized the signal and allowed data acquisition.

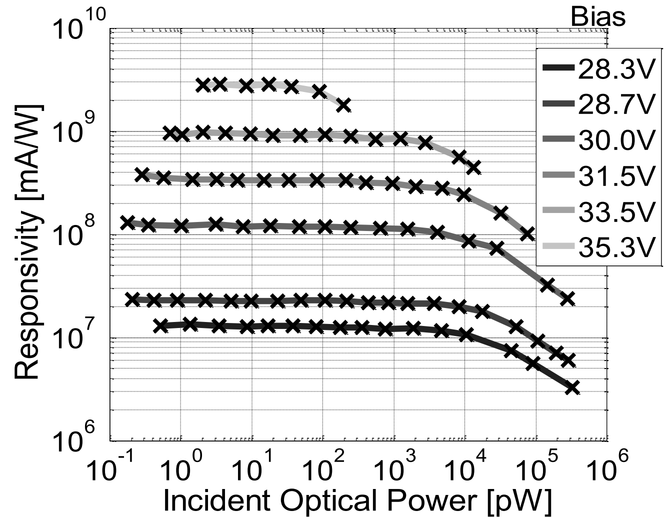

Fig. 6. SiPM responsivity versus incident optical power at $\lambda = 632.8$ nm and at different reverse bias voltages.

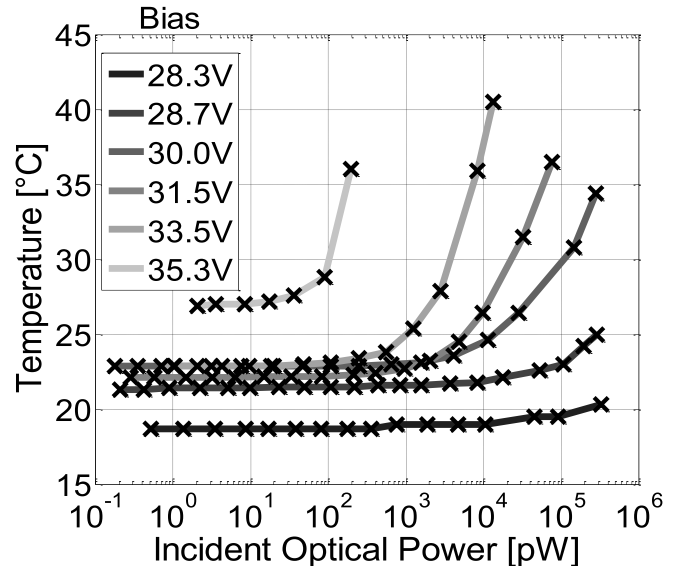

Fig. 7. Temperature of the SiPM package versus incident optical power at $\lambda = 632.8$ nm and at different reverse bias voltages.

The setup described above was the same for the whole duration of the tests, ensuring that all the experiments were reproducible and all data consistent to each other. We biased the SiPM at increasing external bias and we found the responsivity peak (i.e., maximum output current, net of the dark current) applying a reverse bias of 35.3 V between the cathode and the anode. Responsivity measurements were performed at a controlled room temperature and are shown in Fig. 6, while the trend of the temperature of the SiPM package as a function of the incident optical power is shown in Fig. 7.

It is worth noting that responsivity shows a flat response up to a power level, which depends on the applied bias. In more detail, the linear behavior of the device extends up to about 10 nW for a bias of 28.3 V, while it is reduced when the reverse bias voltage increases. In the flat region of each curve, the measured temperature of the SiPM package was

approximately constant (around room temperature), while it increases in the region corresponding to the slope of the curves (Fig. 7). This temperature difference is quite small for lower biases ($\Delta T < 2$ °C for a bias of 28.3 V and $\Delta T < 4$ °C for a bias of 28.7 V) while it strongly increases for higher bias voltages ($\Delta T \approx 18$ °C for a bias of 33.5 V).

We also repeated the measurement at 28.3 V (corresponding to the maximum flat response) reducing the value of the sensing resistor to 50 Ω, to ensure that the SiPM linear response is not influenced by its value. We confirmed that the responsivity turnover occurs at the same optical power.

All the errors were considered and propagated, although the dominant contribution came from the indetermination of the PMT calibration curve (calibration uncertainty = 5%). Measurements were carried out using a battery power supply, to remove possible power line interferences. As above, SiPM output currents, used to evaluate the responsivity, are net of the dark current. In particular, the PMT dark current was negligible in all the performed measurements, while the SiPM dark current was automatically discarded by the lock-in amplifier since it is not chopped.

As previously observed, the linear range extends up to about 10 nW for a bias of 28.3 V. This result considers a maximum deviation of 15% from the linear trend, detected at low incident powers (<10 pW). The linear range is strongly reduced at increasing biases (up to 100 pW at 35.3 V).

Measurements of responsivity as a function of the incident optical power can be explained as follows. The sum of the photon rate and the dark rate in the flat regions are low enough to permit every SiPM cell to quench the avalanche pulse and recharge its diode capacitances (through its quenching resistor) before the same cell is fired again (because another photon hits it again or because a dark event occurs; details about the SiPM electrical model can be found in [31]). Fig. 8 shows the SiPM responsivity versus the rate of firing cells (obtained dividing the SiPM overall current, sum of the dark current and the photocurrent, by the product of the SiPM gain and the elementary charge) for this class of SiPMs, at $\lambda = 632.8$ nm and at different reverse bias voltages. We observe the responsivity turnover occurs at the same value except for the 35.3 V bias. This shows that the responsivity is mainly limited by the finite number of cells that are fired by both photon rate and dark rate, up to the bias of 33.5 V.

At the lowest biases (i.e., 28.3 and 28.7 V), in correspondence to 10 nW, the dark current is very low (the photon current is about 100% of the overall current) and the responsivity begins to decrease mainly because of a pile up effect of the incoming photons during the recharging phase of the SiPM microcells. During this time, the device is not completely blind to the absorption of photons, but it is able to detect the incident light—after the quenching of each avalanche event—showing a triggering efficiency and a gain directly proportional to the overvoltage (OV) at the junction. The amount of charge produced by the microcells, when fired by photons absorbed during the recharging time, is lower than that delivered when the recharging at the depletion layer is complete. Furthermore, for high impinging photon fluxes, the probability that photons can be absorbed by microcells in the recharging phase is

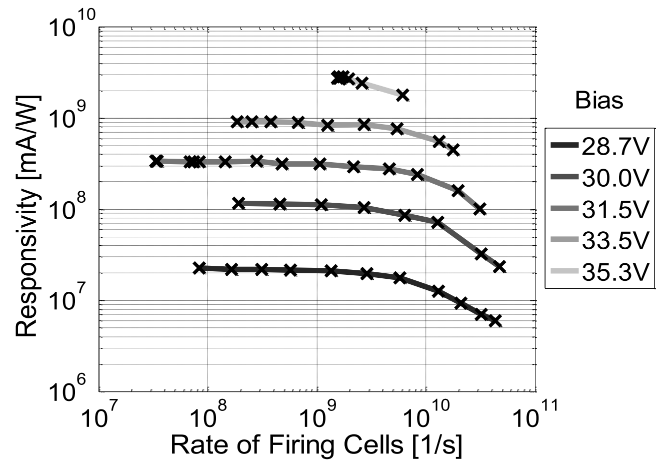

Fig. 8. SiPM responsivity versus rate of firing cells for this class of SiPMs, at $\lambda = 632.8$ nm and at different reverse bias voltages.

higher, due to the limited number of cells in the array. The combination of these effects gives rise to the saturation of the output current that leads to the responsivity decrease, as shown in the curves at 28.3 and 28.7 V (Fig. 6).

Increasing the bias (from 30.0 to 33.5 V), we observed the rise of the dark current due to the rise of the temperature of the SiPM package. The latter is caused by the increase of the waste power that is particularly evident at the highest incident optical powers (in correspondence to the responsivity slopes), as shown in Fig. 7. The photon current decreases down to 82.6% of the overall current, in correspondence to the turnover at 33.5 V. The rise of the dark current, mainly caused by thermal noise, busies the limited number of the SiPM cells and represents the main cause of the early responsivity decrease at the highest biases up to 33.5 V.

Furthermore, as the optical power increases, the photocurrent linearly grows because of the SiPM high gain. As a consequence, the device temperature increases (Fig. 7), thus raising the breakdown voltage with a measured rate of about 30 mV/°C. This measurement was performed locating the SiPM in a black box (dark conditions) and employing a semiconductor parameter analyzer (Keithley 2440). The atmosphere inside the black box was dried using silica gel. The temperature of the SiPM package was controlled through a Peltier cell, placed in the back side of the device, and monitored through a PT100 thermistor.

The growth of the breakdown voltage corresponds to a lower OV on the junction that leads to a gain (and hence responsivity) reduction. The measured shift of the breakdown voltage, in correspondence of the responsivity turnover and considering the lowest measured temperature (19 °C) as the reference temperature, is only about 300 mV at 35.3 V (worst case) and absolutely negligible (less than 1 mV) at 28.3 V (best case). Anyway, this is a secondary effect that could not only explain the responsivity turnover.

Responsivity at 35.3 V was measured up to 200 pW. This curve represents a critical condition for the device in terms of dark current [Fig. 4(a)] and temperature (Fig. 7). The percentage of the overall current due to the photon rate,

in correspondence to the responsivity turnover at 35.3 V, is only 13.6%, very low if compared with the one measured at lower biases. The responsivity turnover at 35.3 V is not aligned to those at the other biases (Fig. 8) because of the strong increase of the current flowing through the junction: indeed, this current is too high to ensure quenching. For this reason, the device is working outside of the usual operation range, i.e., when the quenching resistors sufficiently limit the current during breakdown.

We also estimated the average number of fired cells N_t corresponding to a responsivity deviation of 20% from the linear trend, to make a comparison with the pulsed mode, as in [33]. N_t was obtained as the ratio of the overall average current supplied by the SiPM and the current corresponding to the single SPAD pulse. We found the same value ($N_t \approx 1500$) for all the biases, with the only exception of the 35.3 V bias. This further supports the idea that the responsivity is limited by the dynamic range (number of cells) of the SiPM up to 33.5 V and that the turnover condition occurs when about 42% of cells are fired. This condition is quite close to the common definition of the maximum usable range of SiPM in pulsed mode, i.e., when 50% of cells are fired [33]. A more practical parameter to define this usable range in the CW regime is the maximum ratio of the overall current and the applied OV. For our device this parameter resulted around 0.6 mA/V.

The measured dependence of the responsivity with respect to the incident optical power permits to use the SiPM as a very sensitive power meter with a dynamic range from sub picowatts to several nanowatts, for lower reverse biases [23]. This is an outstanding feature that can be exploited, for example, in those medical imaging systems where such a huge dynamic range is mandatory, being the detected optical power significantly variable with the distance between the detector and the source [29].

C. Spectral Characterization

To evaluate the SiPM responsivity on a broad spectrum and at different bias voltages, we used the setup in Fig. 9. The white light coming out from a xenon lamp was attenuated via a circular variable neutral density filter and spectrally filtered by a monochromator. The output monochromatic light was sent to the SiPM under test or to the reference PMT, according to the position of a flipping mirror placed inside the monochromator and controlled via software. As in the case of measurements reported in the previous section, the SiPM and its biasing circuit were located in a metal black box and a lock-in amplifier was used to reduce noise. To obtain a uniform illumination of the SiPM active area, we set the slit widths of the monochromator at 1 mm (corresponding to a spectral resolution of about 2 nm) and used a 25-mm focal length lens. Spectral measurements were performed from 340 to 820 nm, with a wavelength step of 2 nm.

The attenuated optical power of the xenon lamp, incident on both the PMT and the SiPM, spanned over the 60–100-pW range, to let the SiPM work in the linear region (see Fig. 6). We employed some narrowband filters (full-width at half-maximum = 10 nm) placed in front of the exit slits, to verify that second orders of unwanted light (diffracted by the grating in the same position) were negligible and did not invalidate our measurements.

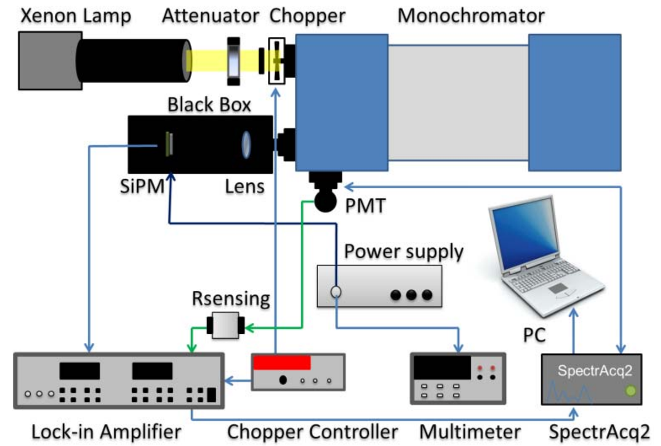

Fig. 9. Sketch of the experimental setup for measurements of SiPM responsivity versus wavelength.

Responsivity was calculated dividing the SiPM photogenerated current by the incident optical power, the latter being estimated from the calibrated PMT photogenerated current. The same considerations concerning the dark current reported in Section III-B apply: it was negligible for the PMT, while it was automatically discarded by the lock-in amplifier for the SiPM.

In Fig. 10(a), we report our responsivity measurements, carried out in the above-mentioned spectral range and at different reverse bias voltages, showing a peak around 669 nm. As expected, we found the highest values of responsivity for the same bias reported in Section III-B (35.3 V) with a maximum value of about $2.9 \cdot 10^9$ mA/W. In Fig. 10(b), we also show the same responsivity measurements, normalized at their values at 669 nm, to better highlight how the spectral shape changes at different biases.

The measured wavelength dependence of the SiPM responsivity can be explained as follows. Most of the power in the blue light range is absorbed within the first 200 nm of silicon, i.e., most of the photons in this range are absorbed in the quasi-neutral region (about 150-nm thick) above the depletion region of the device. Only some of the holes produced by the blue photons diffuse into the high field region and trigger the avalanche with a considerably lower probability than for an electron. The responsivity peak is in the red light range, because of the contribution—to the total measured signal—of the minority carriers (i.e., the electrons) photogenerated in the p-doped epitaxial layers below the junction depletion layer (down to about 3 μm). These carriers can drift toward the lower edge of the depletion layer before being accelerated by the electrical field and, in case, trigger the avalanche pulse. It is well known that the electrons in silicon have a higher diffusivity and impact ionization rates than holes and this makes noteworthy their contribution to the measured signal. In Fig. 10(b), we observe that the responsivity remains substantially unchanged at increasing bias voltages, with a

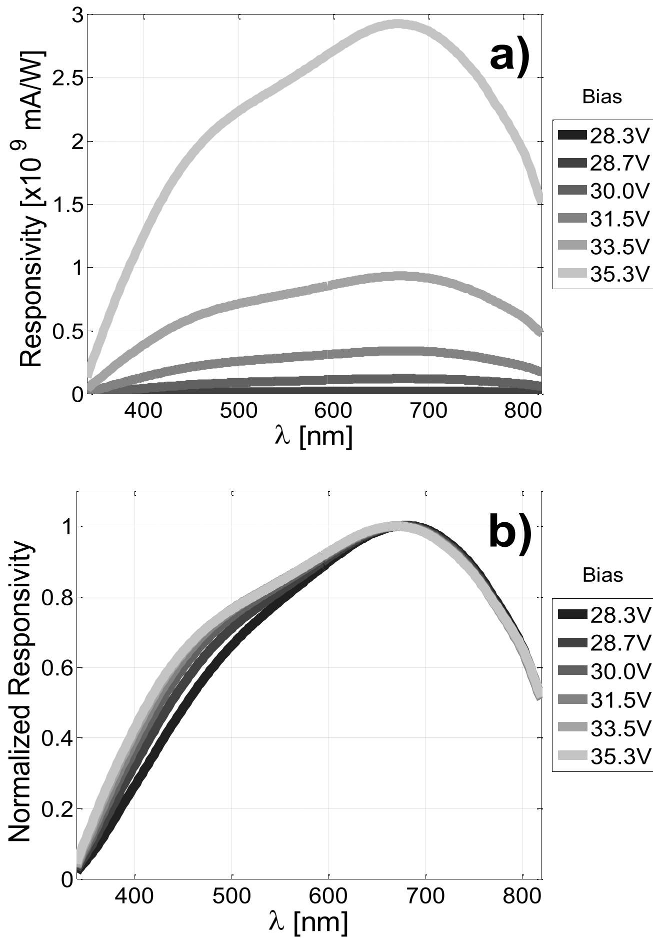

Fig. 10. (a) SiPM responsivity versus wavelength at different reverse bias voltages. (b) Same curves of (a), each one normalized at its value at 669 nm.

slight increase in the blue range. At increasing biases the depletion region of each SPAD widens in the n-doped layer, being the p-doped layer fully depleted once the cell is biased above the breakdown. The spectral changes in the blue are due to a decreasing thickness of the N^+ poly layer. Thus, more holes have a chance to get into the avalanche region and, above all, the probability that these holes produce a breakdown increases.

Light in the near infrared range penetrates deeper into the nondepleted bulk, reducing the probability of reaching the depletion region due to the higher recombination (typical diffusion lengths are $\approx$10 μm) [34]–[36]. The responsivity increases with the bias voltage in the linear region of the reverse I–V characteristic [Fig. 4(a)], while it decreases in the saturation region (i.e., reverse bias above 35.3 V) because of the strong rise of the dark current (curves are not shown).

Such a responsivity response, together with low cost, low supply voltage, high gain, and low noise of the SiPMs, makes them good candidates for a variety of applications (e.g., oximetry and immunoassay).

IV. Conclusion

In this paper, we reported the electrical and optical characterization, in CW regime, of a novel 3600 channels SiPM fabricated on a silicon p-type substrate. In particular we showed, for the first time, a SiPM responsivity measurement as a function of the incident optical power from hundreds of nanowatts down to sub picowatts, at $\lambda = 632.8$ nm, monitoring the device package temperature. We found that responsivity exhibits a flat region whose extension depends on the applied reverse bias voltage. The linear behavior of the device extends up to about 10 nW for the lowest applied bias (28.3 V), while it is reduced when the reverse bias voltage increases. We demonstrated that, up to a bias of 33.5 V, the responsivity decreases because of the limited number of cells that are fired by the photon rate and the dark rate. At higher biases other phenomena occur, thus further reducing the linear range.

The maximum responsivity was measured at a reverse bias voltage of 35.3 V and reaches a value of about $2.9 \cdot 10^9$ mA/W. This result shows the outstanding performances of the fabricated SiPM even at very low photon fluxes and low bias voltages. Moreover, responsivity measurements on a broad spectrum and at different reverse bias voltages were shown: we found the responsivity peak around 669 nm.

A physical interpretation of all the responsivity results was also provided.

References

[1] F. Zappa, S. Tisa, A. Tosi, and S. Cova, "Principles and features of single-photon avalanche diode arrays," *Sens. Actuators A, Phys.*, vol. 140, no. 1, pp. 103–112, Oct. 2007.

[2] G. Collazuol, G. Ambrosi, M. Boscardin, F. Corsi, G. F. Dalla Betta, A. Del Guerra, N. Dinu, M. Galimberti, D. Giulietti, L. A. Gizzi, L. Labate, G. Llosa, S. Marcatili, F. Morsani, C. Piemonte, A. Pozza, L. Zaccarelli, and N. Zorzi, "Single photon timing resolution and detection efficiency of the IRST silicon photo-multipliers," *Nuclear Instrum. Methods Phys. Res. A*, vol. 581, nos. 1–2, pp. 461–464, Aug. 2007.

[3] P. Buzhan, B. Dolgoshein, L. Filatov, A. Ilyin, V. Kantzerov, V. Kaplin, A. Karakash, F. Kayumov, S. Klemin, E. Popova, and S. Smirnov, "Silicon photomultiplier and its possible applications," *Nuclear Instrum. Methods Phys. Res. A*, vol. 504, nos. 1–3, pp. 48–52, Mar. 2003.

[4] V. Golovin and V. Saveliev, "Novel type of avalanche photodetector with Geiger mode operation," *Nuclear Instrum. Methods Phys. Res. A*, vol. 518, nos. 1–2, pp. 560–564, Feb. 2004.

[5] M. Mazzillo, G. Condorelli, D. Sanfilippo, G. Valvo, B. Carbone, G. Fallica, S. Billotta, M. Belluso, G. Bonanno, L. Cosentino, A. Pappalardo, and P. Finocchiaro, "Silicon photomultiplier technology at STMicroelectronics," *IEEE Trans. Nuclear Sci.*, vol. 56, no. 4, pp. 2434–2442, Aug. 2009.

[6] M. Mazzillo, G. Condorelli, D. Sanfilippo, A. Piazza, G. Valvo, B. Carbone, G. Fallica, A. Pappalardo, L. Cosentino, P. Finocchiaro, M. Corselli, G. Suriani, S. Lombardo, S. Billotta, M. Belluso, and G. Bonanno, "Silicon photomultipliers for nuclear medical imaging applications," *Proc. SPIE*, vol. 7003, pp. 70030I-1–70030I-11, Apr. 2008.

[7] M. Mazzillo, A. Piazza, G. Condorelli, D. Sanfilippo, G. Fallica, S. Billotta, M. Belluso, G. Bonanno, L. Cosentino, A. Pappalardo, and P. Finocchiaro, "Quantum detection efficiency in geiger mode avalanche photodiodes," *IEEE Trans. Nuclear Sci.*, vol. 55, no. 6, pp. 3620–3625, Dec. 2008.

[8] V. D. Kovaltchouk, G. J. Lolos, Z. Papandreou, and K. Wolbaum, "Comparison of a silicon photomultiplier to a traditional vacuum photomultiplier," *Nuclear Instrum. Methods Phys. Res. Sec. A, Accel., Spectrometers, Detectors Assoc. Equip.*, vol. 538, nos. 1–3, pp. 408–415, Feb. 2005.

[9] B. Dolgoshein, V. Balagura, P. Buzhan, M. Danilov, L. Filatov, E. Garutti, M. Groll, A. Ilyin, V. Kantserov, V. Kaplin, A. Karakash, F. Kayumov, S. Klemin, V. Korbel, H. Meyer, R. Mizuk, V. Morgunov, E. Novikov, P. Pakhlov, E. Popova, V. Rusinov, F. Sefkow, E. Tarkovsky, and I. Tikhomirov, "Status report on silicon photomultiplier development and its applications," *Nuclear Instrum. Methods Phys. Res. A, Accel., Spectrometers, Detectors Assoc. Equip.*, vol. 563, no. 2, pp. 368–376, Jul. 2006.

[10] D. Renker, “Geiger-mode avalanche photodiodes, history, properties and problems,” *Nuclear Instrum. Methods Phys. Res. A*, vol. 567, no. 1, pp. 48–56, Nov. 2006.

[11] P. Finocchiaro, A. Pappalardo, L. Cosentino, M. Belluso, S. Billotta, G. Bonanno, B. Carbone, G. Condorelli, S. Di Mauro, G. Fallica, M. Mazzillo, A. Piazza, D. Sanfilippo, and G. Valvo, “Characterization of a novel 100-channel silicon photomultiplier—Part I: Noise,” *IEEE Trans. Electron Devices*, vol. 55, no. 10, pp. 2757–2764, Oct. 2008.

[12] P. Finocchiaro, A. Pappalardo, L. Cosentino, M. Belluso, S. Billotta, G. Bonanno, B. Carbone, G. Condorelli, S. Di Mauro, G. Fallica, M. Mazzillo, A. Piazza, D. Sanfilippo, and G. Valvo, “Characterization of a novel 100-channel silicon photomultiplier—Part II: Charge and time,” *IEEE Trans. Electron Devices*, vol. 55, no. 10, pp. 2765–2773, Oct. 2008.

[13] G. Barbarino, R. de Asmundis, G. De Rosa, C. M. Mollo, S. Russo, and D. Vivolo, *Silicon Photo Multipliers Detectors Operating in Geiger Regime: An Unlimited Device for Future Applications*. Vukovar, Croatia: InTech, Jul. 2011.

[14] M. Mazzillo, G. Condorelli, D. Sanfilippo, G. Valvo, B. Carbone, A. Piana, G. Fallica, A. Ronzhin, M. Demarteau, S. Los, and E. Ramberg, “Timing performances of large area silicon photomultipliers fabricated at STMicroelectronics,” *IEEE Trans. Nuclear Sci.*, vol. 57, no. 4, pp. 2273–2279, Aug. 2010.

[15] A. Rochas, A. R. Pauchard, P.-A. Besse, D. Pantic, Z. Prijic, and R. S. Popovic, “Low-noise silicon avalanche photodiodes fabricated in conventional CMOS technologies,” *IEEE Trans. Electron Devices*, vol. 49, no. 3, pp. 387–394, Mar. 2002.

[16] N. Efthimiou, G. Argyropoulos, G. Panayiotakis, M. Georgiou, and G. Loudos, “Initial results on SiPM performance for use in medical imaging,” in *Proc. IEEE Int. Conf. IST*, Jul. 2010, pp. 256–260.

[17] D. J. Herbert, V. Saveliev, N. Belcari, N. D’Ascenzo, A. Del Guerra, and A. Golovin, “First results of scintillator readout with silicon photomultiplier,” *IEEE Trans. Nuclear Sci.*, vol. 53, no. 1, pp. 389–394, Feb. 2006.

[18] P. Buzhan, B. Dolgoshein, L. Filatov, A. Ilyin, V. Kaplin, A. Karakash, S. Klemin, R. Mirzoyan, A. N. Ottec, E. Popova, V. Sosnovtsev, and M. Teshima, “Large area silicon photomultipliers: Performance and applications,” *Nuclear Instrum. Methods Phys. Res. A, Accel., Spectrometers, Detectors Assoc. Equip.*, vol. 567, no. 1, pp. 78–82, Jun. 2006.

[19] E. Roncali and S. R. Cherry, “Application of silicon photomultipliers to positron emission tomography,” *Ann. Biomed. Eng.*, vol. 39, no. 4, pp. 1358–1377, Feb. 2011.

[20] D. Contini, A. Torricelli, A. Pifferi, L. Spinelli, P. Taroni, V. Quaresima, M. Ferrari, and R. Cubeddu, “Multichannel time-resolved tissue oximeter for functional imaging of the brain,” *IEEE Trans. Instrum. Meas.*, vol. 55, no. 1, pp. 85–90, Feb. 2006.

[21] M. Nitzan and H. Taitelbaum, “The measurement of oxygen saturation in arterial and venous blood,” *IEEE Instrum. Meas. Mag.*, vol. 11, no. 3, pp. 9–15, Jun. 2008.

[22] E. Matveeva, J. Malicka, I. Gryczynski, Z. Gryczynski, and J. R. Lakowicz, “Multi-wavelength immunoassays using surface plasmon-coupled emission,” *Biochem. Biophys. Res. Commun.*, vol. 313, no. 3, pp. 721–726, Jan. 2004.

[23] P. Eraerds, M. Legré, A. Rochas, H. Zbinden, and N. Gisin, “SiPM for fast photon-counting and multiphoton detection,” *Opt. Exp.*, vol. 15, no. 22, pp. 14539–14549, Oct. 2007.

[24] M. Cherchi, A. Taormina, A. C. Busacca, R. L. Oliveri, S. Bivona, A. C. Cino, S. Stivala, S. R. Sanseverino, and C. Leone, “Exploiting the optical quadratic nonlinearity of zinc-blende semiconductors for guided-wave terahertz generation: A material comparison,” *IEEE J. Quantum Electron.*, vol. 46, no. 3, pp. 368–376, Mar. 2010.

[25] N. Dinu, K. L. Suh, R. R. Ansari, and L. Rovati, “Electro-optical characterization of SiPM: A comparative study,” *Nuclear Instrum. Methods Phys. Res. A*, vol. 610, no. 1, pp. 423–426, Oct. 2009.

[26] D. Haensse, “A new multichannel near infrared spectrophotometry system for functional studies of the brain in adults and neonates,” *Opt. Exp.*, vol. 13, no. 12, pp. 4525–4538, Jun. 2005.

[27] F. Zou, C. Jin, R. R. Ross, and B. Soller, “Investigation of spectral interferences on the accuracy of broadband CW-NIRS tissue SO_2 determination,” *Biomed. Opt. Exp.*, vol. 1, no. 3, pp. 748–761, Oct. 2010.

[28] G. Salvatori, K. I. Suh, R. R. Ansari, and L. Rovati, “Instrumentation and calibration protocol for a continuous wave near infrared hemoximeter,” *IEEE Trans. Instrum. Meas.*, vol. 55, no. 4, pp. 1368–1376, Aug. 2006.

[29] K. J. Kek, R. Kibe, M. Niwayama, N. Kudo, and K. Yamamoto, “Optical imaging instrument for muscle oxygenation based on spatially resolved spectroscopy,” *Opt. Exp.*, vol. 16, no. 22, pp. 18173–18187, Oct. 2008.

[30] R. Pernice, G. Adamo, S. Stivala, A. Parisi, A. Busacca, D. Spigolon, M. A. Sabatino, L. D’Acquisto, and C. Dispenza, “Opals infiltrated with a stimuli-responsive hydrogel for ethanol vapor sensing (periodical style-accepted for publication),” *Opt. Mater. Exp.*, vol. 3, no. 10, 2013.

[31] G. Condorelli, D. Sanfilippo, G. Valvo, M. Mazzillo, D. Bongiovanni, A. Piana, B. Carbone, and G. Fallica, “Extensive electrical model of large area silicon photomultipliers,” *Nucl. Instrum. Methods Phys. Res. A, Accel., Spectrometers, Detectors Assoc. Equip.*, vol. 654, no. 1, pp. 127–134, Feb. 2011.

[32] F. Corsi, C. Marzocca, A. Perrotta, A. Dragone, M. Foresta, A. Del Guerra, S. Marcatili, G. Llosa, G. Collazzuol, G.-F. Dalla Betta, N. Dinu, C. Piemonte, G. U. Pignatel, and G. Levi, “Electrical characterization of silicon photo-multiplier detectors for optimal front-end design,” in *Proc. IEEE Nuclear Sci. Symp. Conf. Rec.*, Nov. 2006, pp. 276–1280.

[33] D. Renker and E. Lorenz, “Advances in solid state photon detectors,” *J. Instrum.*, vol. 4, no. 4, pp. 1–54, Apr. 2009.

[34] H.-G. Moser, S. Hass, C. Merck, J. Ninkovic, R. Richter, G. Valceanu, N. Otte, M. Teshima, R. Mirzoyan, P. Holl, and C. Koitsch, “Development of back illuminated SiPM at the MPI semiconductor laboratory,” in *Proc. Int. Workshop New Photon-Detectors*, Jun. 2007, pp. 1–7.

[35] G. Adamo, D. Agrò, S. Stivala, A. Parisi, C. Giaconia, A. Busacca, M. C. Mazzillo, D. Sanfilippo, and P. G. Fallica, “Responsivity measurements of N-on-P and P-on-N silicon photomultipliers in the continuous wave regime,” *Proc. SPIE*, vol. 8629, pp. 86291A-1–86291A-9, Mar. 2013.

[36] J. Ninkovic, “Recent developments in silicon photomultipliers,” *Nucl. Instrum. Methods Phys. Res. A, Accel., Spectrometers, Detectors Assoc. Equip.*, vol. 580, no. 2, pp. 1020–1022, Oct. 2007.

Gabriele Adamo received the M.Sc. degree in electronic engineering from the University of Palermo, Palermo, Italy, in 2009.

He is currently attending a Ph.D. program. His current research interests include optical measurements on silicon photomultipliers.

Diego Agrò received the Laurea degree (*cum laude*) in electronic engineering from the University of Palermo, Palermo, Italy, in 2011.

He is currently involved in the development of SiPM-based medical instruments in collaboration with STMicroelectronics.

Salvatore Stivala received the M.Sc. degree in electronic engineering from the University of Palermo, Palermo, Italy, in 2004.

He is currently a Temporary Researcher with the Faculty of Engineering, University of Palermo.

Antonino Parisi received the M.Sc. degree in electronic engineering from the University of Palermo, Palermo, Italy, in 2000.

He is currently a Post-Doctoral Research Fellow with the Faculty of Engineering, University of Palermo.

Giuseppe Costantino Giaconia received the Laurea degree in electronic from the University of Palermo, Palermo, Italy, in 1989.

His current research interests include optoelectronics, nanotechnologies, and digital electronics systems.

Alessandro Busacca received the Ph.D. degree from the University of Palermo, Palermo, Italy, in 2001.

He has been an Associate Professor of electronics with the University of Palermo since 2011.

Massimo Mazzillo received the M.S. degree in physics from the University of Bari, Bari, Italy, in 2002.

He has been with Research and Development, IMS, STMicroelectronics, Catania, Italy, since 2002, where he is currently a Staff Technology Development Engineer.

Delfo Sanfilippo received the M.S. degree in physics from the University of Catania, Catania, Italy, in 1993.

He has been with Research and Development, IMS, STMicroelectronics, Catania, since 1996, as a Researcher of integrated circuit technology development.

Giorgio Fallica received the M.S. degree in physics from the University of Catania, Catania, Italy, in 1978.

He is currently the Manager of the Sensors Design Group, Research and Development, IMS, STMicroelectronics, Catania.